Photocatalytic Behavior of Fe_2O_3, SiO_2, TiO_2, and TiO_2/SiO_2, Fe_2O_3/SiO_2 Core–Shell Nanoparticles towards Decomposition of Methylene Blue

A.M. Ismail[1], M.H. Khedr[2] and M.F. Abadir*[1]

[1]Chemical Engineering Department, Faculty of Engineering, Cairo University
[2]Department of Chemistry, Faculty of science, Beni Suef University
*magdi.abadir@yahoo.com

Abstract: Fe_2O_3, SiO_2, TiO_2 and TiO_2/SiO_2, Fe_2O_3/SiO_2 core–shell nano particles were used to decompose methylene blue (MB) in a laboratory scale study prior to its use in the treatment of waste containing azo dyes that may potentially pose adverse environmental consequences and health hazard to human.
The preparation of TiO_2, Fe_2O_3 cores produced perfectly spherical and smooth surfaces of associated silica shells. The percent degradation of Methylene blue (MB) was measured and found to reach 98% using SiO_2 in 300 min. The corresponding percent degradation using TiO_2 and TiO_2/SiO_2 reached 95% and 81% respectively for the same time period. The results obtained using Fe_2O_3 and Fe_2O_3/SiO_2 core–shell particles were not encouraging.
[A.M. Ismail, M.H. Khedr and M.F. Abadir **Photocatalytic Behavior of Fe_2O_3, SiO_2, TiO_2, and TiO_2/SiO_2, Fe_2O_3/SiO_2 Core–Shell Nanoparticles towards Decomposition of Methylene Blue**. Journal of American Science 2011; 7(10):797 -803]. (ISSN: 1545-1003). http://www.americanscience.org.

Keywords: methylene blue – core shell – nanoparticles - catalysts

1. Introduction

Fifteen percent of the azo dyes used in the textile, paper, leather, ceramic, ink, cosmetics and food processing industries are lost during production and application as wastes [(1)]. The waste containing these dyes may pose adverse environmental consequences and health hazards to humans since it may lead to the formation of carcinogenic aromatic amines when degrading under anaerobic conditions [(2)]. Various options have been be employed to treat such wastes. These include chemical treatment such as chlorination and ozonation [(3,4)], electrochemical treatment [(5)],physical treatment such as adsorption by activated carbon and membranes [(6,7)], photocatalysis [(2)], biological treatment and a combined chemical–biological method [(8)]. The use of semiconducting materials such as SiO_2–TiO_2 as a catalyst [(9)] and Fe_3O_4–TiO_2 as a photocatalyst [(10)] for various chemical reactions are well received due to their unique optoelectronic and photocatalytic properties [(11,12)]. For the decomposition of dyes, silica (SiO_2) was considered in a previous effort due to its stability as a support in solution [(13)]; also the catalytic properties of titania (TiO_2) were exploited in order to decompose organic pollutants in wastewater [(10)].

Despite the favorable properties of titania in the decomposition of dyes, it is not thermally stable when applied independently in a powdered form. This is further exacerbated by the fact that the powdered titania tends to dissolve and lose its surface area readily in the solution, making recovery of TiO_2 catalyst difficult if not impossible. Many researchers, in their effort to improve the stability of titania and enhance the separation of the catalyst from solution, attempted at depositing titania onto the surface of magnetic cores [(14)] while others were interested in depositing titania onto the surface of silica cores due to economic reasons [(15)] . The deposition of titania onto the surface of SiO_2 support cores was achieved by several approaches namely impregnation, precipitation and sol– gel techniques [(16, 17)]. For the applications as catalysts and adsorbents, it is imperative that a proper thickness of TiO_2 film with well-defined textural morphology be developed in order to effect the desired reactions. The proper thickness of titania film may be achieved by increasing the concentration of the titania precursor.

The catalytic activity of titania and iron oxide nanoparticles can be enhanced or suppressed by coating them with appropriate materials. The insulating layers like silica (SiO_2) [(18-19)], alumina (Al_2O_3) [(20-22)], or a polymer [(23-24)], are often expected to isolate the titania nanoparticles from the catalyzed components to suppress the catalytic activity of titania nanoparticles.

The use of hematite Fe_2O_3 as a photocatalyst has also been studied because it is non toxic, abundant, of low cost besides being the most stable form of iron oxide [(25)].

This paper deals first with the preparation and characterization of spherical Fe_2O_3, SiO_2, TiO_2 and TiO_2/SiO_2, Fe_2O_3/SiO_2 core–shell nano-particles. The effectiveness of these core–shell particles in decomposing methylene blue and methyl orange dyes from their aqueous solutions was then tested under different operating conditions and the corresponding kinetics disclosed so as to design high performance materials for water treatment.

Sodium silicate was used as a source of silica because of its low price and to check the ability of relatively low grade silica sources towards methylene blue and methyl orange dyes photodegradation.

Titanium dioxide exists in three different crystalline phases' anatase, rutile and brookite. Anatase was found to be more active photocatalytically than rutile. Due to the large surface area, thin and composite coatings consisting of anatase TiO_2 nanoparticles show high photocatalytic efficiency. The photocatalytic activity of coating TiO_2 do not depend only on the phase, but also on the crystallite size and porosity. For the reasons briefly mentioned above it was interested to check the effect of using TiO_2 rutile phase with and without coating with sodium silicate towards photodegradation

2. Experimental

Materials used for the preparation of the cited nanoparticles were sodium silicate (water glass $Na_2Si_2O_3$, lab. grade) as a source for SiO_2, Titanium dioxide, TiO_2 (II). (Analar grade), Ferric acetate, (Analar grade) as source for Fe_2O_3, Hydrochloric acid (Analar grade) and dionized water (produced by Arab company for pharm. and medical plants-MEPACO- Egypt).

Different spherical nanoparticles were prepared through the following steps:

1. For preparing nano SiO_2, 200 ml of $Na_2Si_2O_3$ and 200 ml water were mixed for 10 min.; 10 ml of HCl were then added and mixing performed for 15 min. then the final mixture was washed with hot deionized water.
2. Cores were prepared by adding 5 g. of core material (Fe_2O_3 or TiO_2) to sodium silicate solution then mixing for 10 min.
3. The presence of unwanted chlorine ions was detected by titration of the washes with silver nitrate solution using potassium chromate and potassium dichromate solution as indicator.
4. The mixtures were then dried at 80°C for one hour.
5. They were then fired for one hour at 300°C in a muffle furnace fitted with an on/off temperature controller. The temperature sensor was a 13% Pt/Pt-Rh thermocouple. The maximum deviation of the thermocouple readings from the set point was ± 5°C at 300°C
6. Nano iron oxide was prepared by heating 250 g. of ferric acetate powder for 48 hours.

3. Characterization

3.1- X-ray Diffraction

Diffraction patterns were obtained by means a chart recording Bruker ax5 –D8 Advance –Diffrax plus search X-ray diffractometer using copper (Kα) radiation.

The interplanar spacings (d) were derived from Bragg's law:

$$2d \sin\theta = n.\lambda, (n=1) \quad (1)$$

where λ =1.5405 Å, is the wavelength associated with the Cu K_α radiation used. The relative intensity (I/I_0) was calculated for all lines in the obtained diffraction patterns.

The average crystallite size was calculated using the diffractions peaks from Scherer's formula

$$D = 0.9 \lambda / (\beta - \beta_1) \cos\theta \quad (2)$$

Where D is the grain diameter in Å, β is the half-intensity width of the relevant diffraction peak, β_1 represents the half-intensity width due to instrumental broadening, λ is the X ray wave length, and θ is the angle of diffraction.

3.2. Photocatalytic activity

Photocatalysis experiments were carried out in 100 ml beaker containing about 100 ml of MB or MO aqueous solution (0.003 gm) and about 0.3 mg of the catalyst at natural pH ≈ 7. Experiments were carried out under two different sets of conditions: direct light, and without light.

Irradiation was carried out using a 200W tungsten lamp as a source of visible light, which was placed vertically on the reaction vessel at a distance of 200 mm. (The operating distance from the filament of the lamp). At specific time intervals, a certain amount of the sample solution was withdrawn and the changes in color concentration of the dye were observed from its characteristic absorption band at around 664 nm using a UV – Vis spectrophotometer model (Jasco V- 530).

The percent degradation of the tested dyes was calculated using the following formula:

$$\text{Percent degradation} = (1- (At / A_{0})) \times 100 \quad (3)$$

Where A_t is the absorbance after time t and A_o is the dye initial concentration before degradation.

4. Results and discussion

4.1- X-Ray and TEM Characteristics

From X-ray measurements using Scherrer equation it was found that the crystallite sizes of all samples were in the nano size range: Fe_2O_3, SiO_2, TiO_2 and TiO_2/SiO_2, Fe_2O_3/SiO_2 for TiO_2 = 106 nm and for Fe_2O_3 = 44 nm

The X-ray diffraction patterns of uncoated iron oxide and titanium oxide particles, silica, silica coated iron oxide and silica coated titanium oxide particles yielded the maximum peak intensities shown in Table (1) with d-values corresponding to peak intensities.

Table 1: XRD Parameters.

Material	2θ	I/I_o	d (Å)
TiO_2	27.5	100	3.24
Fe_2O_3	35.6	100	2.52
TiO_2/SiO_2	27.5	100	3.25
Fe_2O_3/SiO_2	35.7	100	2.51

Pure silica exhibited a highly amorphous structure while strong and sharp peaks indicate the well-crystalline nature of α-Fe_2O_3 and TiO_2 nano crystals in uncoated particles.

The XRD spectrum of coated samples revealed a highly amorphous silica structure and small peaks corresponding to crystalline Fe_2O_3 and TiO_2.

The average crystallite size of Fe_2O_3/SiO_2 particles is lower than that of pure Fe_2O_3 (35 nm compared to 44 nm) as shown by TEM (Fig. 1). This result, together with XRD results, indicates that the addition of SiO_2 decreased the crystallite size and crystallinity by inhibiting the growth of Fe_2O_3 core particles. It is worth noticing that the core particle of Fe_2O_3/SiO_2 particles (44 nm) in diameter (obtained from XRD) is fairly consistent with the crystallite size of 35 nm (obtained from TEM- Fig 1).

A different result was obtained for titania coated particles as coating increased the average crystallite size from 55 nm for pure TiO_2 to 66 nm for SiO_2 coated TiO_2.

For Fe_2O_3 the decrease in volume observed on the formation of core – shell particles with silica mainly reflects the substitution of Fe^{3+} and by Si^{4+} as well as the formation of Fe–O–Si bonds because the radius of Si^{4+} (0.041 nm) is much smaller than that of Fe^{3+} (0.065 nm)

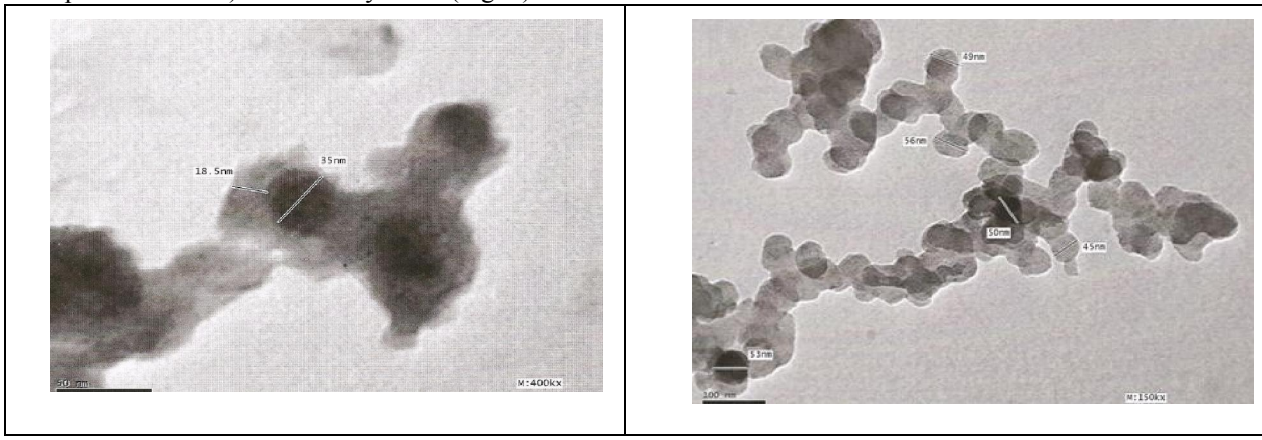

Fig. 1 TEM a: Pure iron oxide **b: Silica coated iron oxide**

4.2. Photocatalytic activity in degradation of MB

The prepared powders were tested as catalysts for the photocatalytic decomposition of methylene blue (MB). The effect of core and shell materials and conditions of decompositions of MB dye was investigated in visible light as well as without light.

The change in the absorbance of MB was recorded as a function of time as shown in Fig.2 .

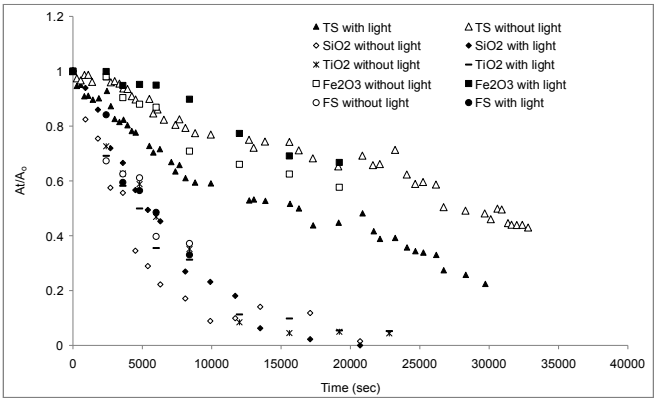

Fig.2 Photodegradation of MB in presence of different nanocatalysts

The rate of degradation is highest at the early stages of reaction and gets slower with time till the end of the reaction. It was observed in the UV – Vis spectrophotometer that the maximum absorption peak at 664 nm corresponding to the azo bond of MB molecule diminished gradually as the irradiation time increased .It disappeared completely after different time intervals depending on core shell materials.

The percent degradation of MB was calculated from equation (3) and the results are shown in table 2.

It can be seen that it is greatly affected by the presence of core–shell particles: MB is 98% decomposed in 300 min using silica nano powders with and without light. For Fe_2O_3/SiO_2 core–shell particles the decomposition reaches 51% with light and 60% without light in 100 min compared to 5% and 13% when pure Fe_2O_3 powder was used.

Using TiO_2/SiO_2 core–shell particles the degradation level was 78 % in 300 min with light and 81% without light compared to 95% when using pure TiO_2.

Accordingly, it can be concluded that the rate of degradation of MB dye increased by coating Fe_2O_3 with SiO_2 because of decreased crystallite size and hence higher surface area and better photocatalytic activity. On the other hand the increase in crystallite size associated with coating of TiO_2 by SiO_2 reflects negatively on the degradation of MB.

It also can be seen that during the first 200 min the degradation of MB increases rapidly slowing afterwards as shown in table 2

Table 2 : Percent Degradation of MB

Powder	Time minute	100	200	300
S	With light	55	82	98
	Without light	78	90	98
T	With light	65	89	95
	Without light	53	92	95
F	With light	5	23	33
	Without light	13	34	43
SF	With light	51	---------	---------
	Without light	60	---------	---------
ST	With light	73	75	78
	Without light	56	65	81

Under light-rich conditions, photocatalytic reaction rate depends on the adsorptive property of MB onto the catalysts surface.

The more the amount of MB adsorbed onto the catalysts surface, the higher the photobleaching rate [27]. As the illumination time increases, the amount of dye adsorbed onto the catalysts surface becomes smaller due to photobleaching of MB by the catalysts [28]. Therefore, the percent degradation of MB increases slowly after the first 200 min.

In case of Fe_2O_3/SiO_2 the transition from Fe^{3+} to Fe^{2+} corresponds to the transition from d^5 to d^6, and Fe^{2+} is relatively unstable due to the loss of exchange energy and tends to return to Fe^{3+}, resulting in the release of the trapped electron becoming easy.

According to Fenton reactive mechanism, the coexistence of Fe^{2+} and H_2O_2 in an acidic condition may produce ·OH, which has strong oxidizing power. Hence, it can be inferred that the following reactions may occur simultaneously in the reactive system.

$$Fe^{3+}+e^{-}\rightarrow Fe^{2+}$$
$$Fe^{2+}+H_2O_2+H^{+}\rightarrow Fe^{3+}+ OH^{-}+H_2O$$
$$Fe^{2+}+HO_2+H^{+}\rightarrow Fe^{3+}+H_2O_2$$
$$H_2O_2+ e^{-}\rightarrow \cdot OH + OH^{-}$$

Therefore the vacancies introduced in the crystal lattice by Fe^{3+} make the surface charges unbalanced. Hence the concentration of hole carriers may increase under visible light irradiation with increasing amount of Fe^{3+} and the photocatalytic efficiency may improve accordingly. Thus, it can be inferred from our experimental results the vacancies in the above crystal play an important role in the improvement of the photocatalytic activity. This is in accordance with the work of Bitao et al. [29] who studied the photocatalytic degradation of methylene blue on Fe^{3+} doped TiO_2 nanoparticles under visible light irradiation.

Comparing SiO_2 to TiO_2/SiO_2 the decrease of titania surface area caused by silica coating caused the photocatalytic activity to decrease; also from XRD it was observed that the titania phase is rutile which was reported to give slower degradation than anatase [30]. Rutile has a little absorption in the visible light region. However, its photocatalytic activity is not high because the photo-generated electron-hole pairs can easily recombine with each other by ultraviolet or visible light. The photo-generated electrons mainly remain in the interior of rutile phase TiO_2, and react easily with TiO^{2+} to produce the Ti^{3+} ions instantly. Subsequently, these Ti^{3+} ions capture photo-generated holes thus generating a side-effect to the photocatalytic reaction [31].

4.3 Kinetics of photocatalytic degradation of MB

In studying the kinetics of degradation of MB, it was first assumed that the reaction follows a first order model. So, a plot of ln (A_t/ A_o) versus time should yield a straight line, the slope of which upon linear regression equals the apparent first-order rate constant K

$$Ln(At/A_{0)}=-K.t \qquad (4)$$

Where A_0 and A_t are absorbance of the dyes at time 0 and at time t respectively. K is the first order rate constant in min^{-1} and t is the time in minutes.

Fig. 3 was drawn for the case of SiO_2 catalyst as an example to show that this assumption is valid. Actually it was found to be valid in most cases except for the degradation of MB with Fe_2O_3 in light and Fe_2O_3/SiO_2 without light that yielded linear fits corresponding to second order reactions following the kinetic equation:

$$\frac{1}{A} = \frac{1}{A_0} - K.t \qquad (5)$$

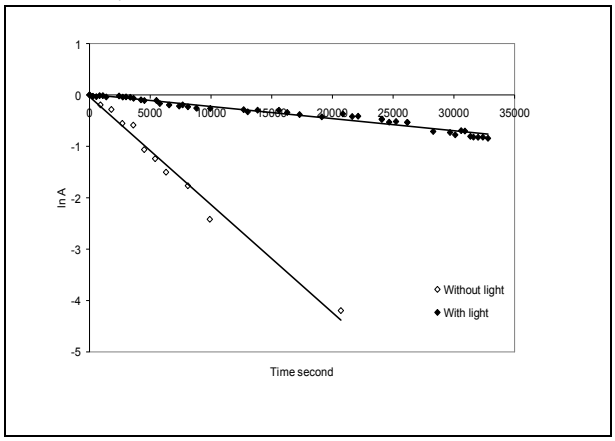

Fig.3 First order kinetics of degradation of MB in presence of SiO_2 catalyst

Fig. 4 shows the second order kinetics for these two cases. Table 3 shows the values of the rate constants obtained in each case together with the corresponding determination coefficient R^2.

Table 3: K and R^2 values for MB degradation

Sample	With light			Without light		
	Order	k	R^2	Order	k	R^2
S	1	0.0086	0.977	1	0.0129	0.990
T	1	0.0088	0.969	1	0.0074	0.992
F	2	0.0018	0.947	1	0.0018	0.955
SF	1	0.0075	0.968	2	0.0125	0.950
ST	1	0.0078	0.968	1	0.0076	0.988

The effect of coating of F and T samples on the kinetics of degradation can be followed up from the previous table where it can be seen that the degradation rate is much faster for Fe_2O_3/SiO_2 samples compared to Fe_2O_3 samples, whether with or without light. This effect did not show in case of T samples where coating did not contribute to increased rate of degradation as can be seen from the relative figures of k in the table. Such result is consistent with the previous section (4.3.1) concerning the role of coating in both F and T samples.

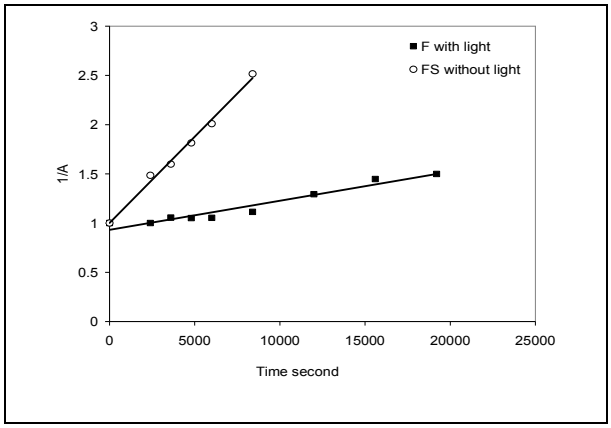

Fig.4 Second order kinetics of degradation of MB in presence of Fe_2O_3 or FS catalyst

Conclusions

Different nanosized powders were used as catalysts for the degradation of Metylene Blue (MB). These were: Fe_2O_3, SiO_2, TiO_2, and TiO_2/SiO_2, Fe_2O_3/SiO_2 core–shell particles. Low cost raw materials were used in preparation. Degradation was studied in absence and in presence of direct light. XRD was used to identify the different phases and to calculate their crystallite size. UV was used to follow the extent of photodegradation. TEM micrographs were used to show the evidence of formation of core shell particles as well as to obtain their mean nanosize.

The following results were obtained:

1. Coating of titania and iron oxide particles with silica yielded smaller nanosizes with improved catalytic action for the degradation of MB.
2. The best degradation results were obtained on using pure silica or titania nanocatalysts whether in presence of or in absence of direct sunlight.
3. The catalytic effect of silica coated titania was higher than that of silica coated iron oxide for MB degradation.
4. Most of degradation reactions of MB using the different catalysts at hand followed first order kinetics.

Corresponding author
M.F. Abadir
Chemical Engineering Department, Faculty of Engineering, Cairo University
magdi.abadir@yahoo.com

References

1. Sokmen M., Allen D.W., Akkas F., Kartal N., Acar F., "Photo-degradation of some dyes using Ag-loaded titaniumdioxide", Water Air Soil Pollution, 132, 2001, pp.153–163.
2. Badr Y., Mahmoud M.A., "Photocatalytic degradation of methyl orange by gold silver nano-core/shell nano-shell", J. Phys. Chem. Sol. 68, 2007, pp.413–419.
3. Slokar Y.M., Le Marechal A.M., "Methods of decoloration of textile waste waters", Dyes and Pigments, 37, 1998, pp.335–339.
4. Gökçen F., Özbelge T.A., "Pre-ozonation of aqueous azo dye (Acid Red-151)followed by activated sludge process", Chem. Eng. J., 123, 2006, pp.109–115.
5. Jain R., Varshney S., Sikarwar S., "Electrochemical techniques for the removal of Reactofix Golden Yellow 3 RFN from industrial wastes", J. Colloids and Interface Sci. ,313, 2007, pp.248–253.
6. Ong S.A., Toorisaka E., Hirata M., Hano T., "Granular activated carbon-bio film configured sequencing batch reactor treatment of C.I. Acid Orange 7", Dyes and Pigments, 76, 2008, pp.142–146.
7. Mozia S., Tomaszewska M., Morawski A.W., "Photodegradation of azo dye Acid Red 18 in a quartz labyrinth flow reactor with immobilized TiO_2 bed", Dyes and Pigments, 75, 2007, pp. 60–66.
8. Lucas M.S., Dias A.A., Sampaio A., Amaral C., Peres J.A., "Degradation of a textile reactive Azo dye by a combined chemical-biological process: Fenton's reagent yeast", Water Res., 41, 2007, pp.1103–1109.
9. Zhou Y., Wei Q., Ma H., Zhang Z., "Y/composite titania–silica (CTS) supported catalyst for hydrotreating coker gas oil", Catalysis Today , 125, 2007, pp.211–219.
10. Beydoun D., Amal R., "Implications of heat treatment on the properties of a magnetic iron oxide–titanium dioxide photocatalyst", Mater. Sci. Eng. B. ,94, 2002, pp. 71–81.
11. Muneer M., Philip R., Das S., "Photocatalytic degradation of waste water pollutants", Research on Chemical Intermediates, 23,1997, pp.233–240.
12. Tang W.Z., Huang C.P., "Stoichiometry of Fenton's reagent in the oxidation of chlorinated aliphatic organic pollutants", Environ. Tech., 18 ,1997, pp.13–23.
13. Zang L., Liu C.Y., Ren X.M., "Photochemistry of semiconductor particles. Part 4. Effects of surface condition on the photodegradation of 2,4-dichlorophenol catalysed by TiO_2 suspensions", J. Chem. Soc., Faraday Trans, 91, 1995 pp.917-925.
14. Fu W., Yang H., Li M., Chang L., Zang L., Liu C.Y., Ren X.M., "Photochemistry of semiconductor particles. Part 4. Effects of surface condition on the photodegradation of 2,4-dichlorophenol catalysed by TiO_2 suspensions",, Q. Yu, J. Xu, G. Zou, Preparation and photocatalytic characteristics of core–shell structure $TiO_2/BaFe_{12}O_{19}$ nanoparticles, Material Letters,Vol.60, (2006) 2723–2727.
15. Lee J.W., Othman M.R., Eom Y., Lee T.G., Kim W.S., Kim J., "The effects of sonification and TiO_2 deposition on the micro-characteristics of the thermally treated SiO_2/TiO_2 spherical core–shell particles for photo-catalysis of methyl orange", Microporous and Mesoporous Materials, 116, (1-3), Dec. 2008, pp. 561-568
16. Hsu W.P., Yu R., Matijevic E., "Paper Whiteners: I. Titania coated silica", J. Colloids and Interface Sci., 156, 1993, pp.56–65.
17. Castillo B. K., Ruiz P., Delmon B., 'Influence of preparation methods on the texture and structure of titania supported on silica", J. Mater. Chem., 4, 1994, pp.903–906.
18. Huang X., Chen Z., "A study of nanocrystalline $NiFe_2O_4$ in a silica matrix", Mater. Res. Bull., 40 ,2005, pp.105–113
19. Mori T., Tanaka K., Inomata T., Takeda A., Kogoma M., "Development of silica coating methods for powdered pigments with atmospheric pressure glow plasma", Thin solid films, 316, (1-2), March 1998, pp.89–92.
20. Cano I.G., Dosta S., Miguel J. R., Guilemany J. M., "Production and characterization of metastable Al_2O_3–TiO_2 ceramic materials" , J. Mater Sci , 42, 2007, pp.9331–9335
21. Linacero R., Rojas-Cervantes M.L., LoPez-González J.D., "Preparation of $xTiO_2.(1-x)Al_2O_3$ catalytic supports by the sol-gel method physical and structural characterization' , J. Mater. Sci., 35, 2000, pp.3279 – 3287
22. Q. H. Powell, G. P. Fotou, T. T. Kodas, B. M. Anderson, "Synthesis of aluminaand alumina/silica-coated titania particles in an aerosol flow reactor", Chem. Mater.,9 (3), 1997, pp.685 -693
23. Fan X., Lin L., Messersmith P.B., "Surface-initiated polymerization from TiO2 nanoparticle surfaces through a biomimetic initiator: A new route toward polymer–matrix nanocomposites" ,Composites Sci. Tech. 66 , 2006, pp.1198–1204
24. Liang H., Li X., "Visible-induced photocatalytic reactivity of polymer–sensitized titania nanotube

films" , Applied Catalysis B: Environ. Sci. Tech. 44 (9), 2010, pp.3481 – 3485.
25. Cherepy N.J., Liston D.B., Lovejoy J.A., Deng H., Zhang J.Z., "Ultrafast studies of photoexcited electron dynamics in γ and α Fe_2O_3 semiconductor nanoparticles", J. Phys. Chem.. B, 102, 1998, pp.770-776
26. Wang L.Y., Sun Y.P., Xu B.S., "Comparison study on the size and phase control of nanocrystalline TiO_2 in three Ti–Si oxide structures", J. Mater. Sci., 43, No. 6 March,2008, pp.1979–1986
27. Miyauchi, A. Nakajima, Watanabe T., Hashimoto K., "Photo induced Hydrophilic Conversion of TiO_2/WO_3 Layered Thin Films", Chem. Mater ,14, 11(Nov. 2002) pp.4714-4720
28. Bitao S., Ke W., Jie B., Hongmei M., Yongchun T., Shixiong M., Shixiong S., Ziqiang L., "Photocatalytic degradation of methylene blue on Fe^{3+} doped TiO_2 nanoparticles under visible light irradiation", Front. Chem. China, 2 (4) , 2007, pp. 364–368
29. Tayadea R. J., Suroliaa P. K., Kulkarnib R. G., Jasra R. V., "Photocatalytic degradation of dyes and organic contaminants in water using nanocrystalline anatase and rutile TiO_2", Sci. Techn. Adv. Mater., 8, 2007, pp.455–462
30. Wang J., Li R., Zhang Z., Sun W., Wang X., R.Xu , Xing Z., Zhang X., "Degradation of Hazardous Dyes in Wastewater using Nanometer Mixed Crystal TiO_2 Powders under Visible Light Irradiation", Water Air Soil Pollut.,189, 2008, pp.225–237.
31. Tada H., Kubo Y., Akazawa M., Ito S., "Promoting Effect of SiO_x Monolayer Coverage of TiO_2 on the Photoinduced Oxidation of Cationic Surfactants", Langmuir , 14 , 1998, pp.2936-2939.

10/12/2011